Published in final edited form as:
Biochem J. 2014 September 1; 462(2): 231–245. doi:10.1042/BJ20131581.

Identification of Protein Succination as a Novel Modification of Tubulin

Gerardo G. Piroli[*], **Allison M. Manuel**[*], **Michael D. Walla**[†], **Matthew J. Jepson**[‡], **Jonathan W.C. Brock**[§], **Mathur P. Rajesh**[‖], **Ross M. Tanis**[*], **William E. Cotham**[†], and **Norma Frizzell**[*,1]

[*]Department of Pharmacology, Physiology & Neuroscience, School of Medicine, University of South Carolina, 6439 Garners Ferry Rd, Columbia, SC 29209, USA

[†]Mass Spectrometry Center, Department of Chemistry & Biochemistry, University of South Carolina, 631 Sumter St, Columbia, SC 29205, USA

[‡]Department of General Surgery, Carolinas Medical Center, 1000 Blythe Boulevard, Charlotte, NC 28203, USA

[§]Department of Pediatrics, School of Medicine, University of South Carolina, 14 Richland Medical Park Columbia, SC 29203, USA

[‖]Department of Chemical Engineering, Kattankulathur Campus, SRM University, Chennai, India

Abstract

Protein succination is a stable post-translational modification that occurs when fumarate reacts with cysteine residues to generate S-(2-succino)cysteine (2SC). We demonstrate that both alpha (α) and beta (β) tubulin are increasingly modified by succination in 3T3-L1 adipocytes and in the adipose tissue of *db/db* mice. Incubation of purified tubulin from porcine brain with fumarate (50 mM) or the pharmacological compound dimethylfumarate (DMF, 500 μM) inhibited polymerization up to 35% and 59%, respectively. Using mass spectrometry we identified Cys347α, Cys376α, Cys12β and Cys303β as sites of succination in porcine brain tubulin and the relative abundance of succination at these cysteines increased in association with fumarate concentration. The increase in succination after incubation with fumarate altered tubulin recognition by an anti-α-tubulin antibody. Succinated tubulin in adipocytes cultured in high glucose vs. normal glucose also had reduced reactivity with the anti-αtubulin antibody; suggesting that succination may interfere with tubulin:protein interactions. DMF reacted rapidly with 11 of the 20 cysteines in the αβ tubulin dimer, decreased the number of free sulfhydryls and inhibited the proliferation of 3T3-L1 fibroblasts. Our data suggests that inhibition of tubulin polymerization is an important, undocumented mechanism of action of DMF. Taken together, our results demonstrate that succination is a novel post-translational modification of tubulin and suggest that

[1]To whom correspondence should be addressed: Norma Frizzell, Department of Pharmacology, Physiology & Neuroscience, School of Medicine, University of South Carolina, 6439 Garners Ferry Road, Columbia, SC 29209, USA, Tel.: (803) 216-3521; Fax: (803) 216-3538; norma.frizze11@uscmed.sc.edu.

Author Contribution: Gerardo Piroli designed and performed experiments, contributed to the discussion and wrote the paper; Allison Manuel performed experiments and analyzed data; Michael Walla performed experiments and analyzed data; Matthew Jepson performed experiments and analyzed data, Jonathan Brock, Mathur Rajesh, Ross Tanis and William Cotham performed experiments; Norma Frizzell designed the experiments, analyzed the data and edited the manuscript prior to submission.

extensive modification by fumarate, either physiologically or pharmacologically, may alter microtubule dynamics.

Keywords

Adipocyte; cysteine; dimethylfumarate; fumarate; microtubule; succinocysteine; succination; tubulin

Introduction

The Krebs cycle metabolite fumarate can react with thiol groups on cysteine residues to generate the stable adduct, S-2-(succino)cysteine (2SC), also termed succination of proteins [1]. We have previously described an increase in fumarate and protein succination in 3T3-L1 adipocytes matured in high glucose medium and in the adipose tissue of type 2 diabetic *db/db* and *ob/ob* mice [2-5], and we have developed a specific anti-2SC polyclonal antibody to detect succinated proteins [2]. Several of the succinated proteins in adipocytes have been identified including cytoskeletal proteins, endoplasmic reticulum chaperones and hormones [2]. The hormone adiponectin has been shown to be succinated both *in vitro* and *in vivo*, preventing its incorporation into high molecular weight oligomers and secretion from the adipocyte [3] and demonstrating the functional impact of succination on a target protein. Protein succination is also increased in the gastrocnemius muscle of 6 month old type 1 diabetic rats and results in a reduction in the activity of the glycolytic enzyme glyceraldehyde-3-phosphate dehydrogenase (GAPDH) [1, 6]. However, the levels of protein succination did not significantly change in the gastrocnemius muscle of 16 week old *db/db* mice, a model of type 2 diabetes [5]. Protein succination appears to be a sensitive biomarker of mitochondrial stress in the white adipocyte [4] and, while 2SC levels were unchanged in other tissues of the *db/db* mouse, a prominent succinated protein ∼50 kDa was consistently detected in both skeletal and cardiac muscle, lungs and adipose tissue [5]. In the present work we have confirmed the identification of this protein, the most abundantly succinated protein by anti-2SC antibody staining in adipocytes, as tubulin.

The α and β isotypes of tubulin form heterodimers that are the building blocks for cytoskeletal microtubules. Several post-translational modifications (PTMs) of tubulin have been described including acetylation, tyrosination, glutamylation, glycylation, phosphorylation and palmitoylation [7-10]. The majority of these PTMs, with the exception of acetylation, have been documented to increase close to the carboxyl termini of α and β tubulins and have diverse roles in regulating microtubule length and stability or the regulation of microtubule associated proteins (MAPs) [7-10]. While all of these PTMs are believed to be enzymatically regulated [7], the non-enzymatic modification of tubulin by nitric oxide, hydrogen peroxide and the lipid peroxidation product 4-hydroxynonenal (4-HNE) has also been described [11-16]. Tubulin carbonylation by 4-HNE is known to target several cysteine residues [15-19], including Cys295α, Cys347α, Cys376α, and Cys303β, resulting in decreased polymerization and increased tubulin cross-linking [16, 17]. The αβ tubulin dimer contains a total of 20 cysteines (12 in α-tubulin and 8 in β-tubulin), 16 of which are rapidly reactive with electrophiles [20]. The reactivity depends on the electrostatic

environment of each individual residue and increases in proximity to positively charged residues that favor the ionization of the thiol group to thiolate [20]. In the present study we describe protein succination as a novel modification of both α and β tubulin under *in vitro* conditions during high glucose culture and in the adipose tissue of *db/db* mice. We also demonstrate that dimethylfumarate (DMF), a more reactive fumarate ester, lowers tubulin polymerization and fibroblast proliferation, suggesting that the pharmacological modification of proteins by succination may have a regulatory role in microtubule dynamics.

Experimental

Chemicals

Unless otherwise noted, all chemicals were purchased from Sigma/Aldrich Chemical Co (St. Louis, MO & Milwaukee, WI). Criterion polyacrylamide gels and Precision Plus protein ladder were purchased from BioRad Laboratories (Richmond, CA). PVDF membrane and ECL Plus chemiluminescent substrate were from GE Healthcare (Piscataway, NJ). The synthesis of 2-succinocysteamine and preparation of polyclonal anti-2SC antibody has been described previously [2]. The following commercial antibodies were used: α-tubulin B-7 from Santa Cruz Biotechnology (Dallas, TX) and DM1A from Cell Signaling Technology, Inc. (Danvers, MA); β-tubulin TUB2.1 from Santa Cruz Biotechnology and D65A4 from Cell Signaling Technology, Inc.; combined αβ-tubulin ATN02 from Cytoskeleton, Inc. (Denver, CO); and actin I-19 from Santa Cruz Biotechnology.

Cell Culture

Murine 3T3-L1 fibroblasts were obtained from the laboratory of Dr. Howard Green (Harvard Medical School, Boston, MA). The cells were maintained as pre-adipocytes or differentiated into adipocytes as described previously [2, 4, 5]. After differentiation, the adipocytes were cultured in Dulbecco's Modified Eagle's Medium (DMEM) containing either 5 mM D-glucose and 0.3 nM insulin or 30 mM D-glucose and 3 nM insulin for an additional period of 4-8 days (maturation period). C2C12 cells were purchased from the American Type Culture Collection (Manassas, VA) and cultured in DMEM supplemented with 10% FBS, 50 U/ml penicillin and 50 μg/ml streptomycin. After reaching confluence, myoblast differentiation was induced for 72 h in DMEM supplemented with 2% heat-inactivated horse serum. For all cells the culture medium was changed every 48 h but glucose was supplemented into the media at 24 h intervals to maintain glucose levels at 5 mM. Preliminary experiments using L-glucose as an osmotic control indicated that it had no effect on increasing protein succination (data not shown). Cells were harvested in radioimmunoprecipitation assay (RIPA) lysis buffer (50 mM Tris-HCl, 150 mM NaCl, 1 mM EDTA, 0.1% Triton X-100, 0.1% sodium dodecyl sulfate (SDS), 0.5% sodium deoxycholate, pH 7.4), with the addition of 2 mM diethylenetetraminepentaacetic acid (DTPA) and a protease inhibitor cocktail (P8340, Sigma Aldrich, St Louis, MO). The cell lysate was pulse sonicated at 2 watts using a Model 100 sonic dismembrator (Fisher Scientific, Fair Lawn, NJ) for 1 min prior to resting on ice for 30 min in lysis buffer. The protein was precipitated with 9 volumes of cold acetone for 10 min on ice. After centrifugation at 3,000 x *g* for 10 min and removal of the acetone, the protein pellet was

resuspended in 500 μl RIPA buffer. The protein content was determined by the Lowry assay [21].

Mouse Tissue Preparation

All experiments with mice were conducted at the University of South Carolina in accordance with protocols approved by the Institutional Review Board or the Institutional Animal Care and Use Committee. Control and *db/db* diabetic mice were purchased from Jackson Laboratories (Bar Harbor, ME). Animals were sacrificed by CO_2 asphyxiation at 15 weeks age and adipose tissue, sciatic nerves and brains were removed immediately, snap frozen in liquid nitrogen and stored at −80°C until use. Tissues used for immunoprecipitation and gel separation procedures were homogenized by sonication in RIPA buffer, and proteins were precipitated with acetone and resuspended as described above (see Cell Culture). Samples were stored at −80°C until use.

Immunoprecipitation

Immunoprecipitation with a monoclonal anti β-tubulin antibody was performed as previously described [6], with minor modifications. Briefly, protein from C2C12 myotubes, 3T3 adipocytes (500 μg) or adipose tissue (200 μg) was diluted to 500 μl with a mix of 50% RIPA buffer/50% PBS, containing 2 mM DTPA and a protease inhibitor cocktail. To decrease non-specific binding, preparations were pre-incubated with non-immune Protein G-coupled agarose beads (Thermo Scientific, Rockford, IL) for 30 min at room temperature with gentle shaking. After a 5 min spin at 3,000 x *g*, 1 μg anti β-tubulin antibody was added to the pre-cleared supernatant and incubated overnight at 4°C with gentle shaking. 10 μl Protein G-coupled agarose beads were incubated with the lysate for an additional 4 h. After a 5 min centrifugation at 3,000 x *g*, the supernatant was removed and the agarose beads were washed in PBS 3 times followed by boiling in Laemmli buffer prior to 1-dimensional or 2-dimensional electrophoresis and western immunoblotting (see below).

One-dimensional PAGE and Western Blotting

Western blotting to probe for protein succination, tubulin and actin was performed as described previously [2]. In some cases, membranes were stripped with 62.5 mM Tris, pH 6.8, containing 2% SDS and 0.7% 2-mercapto ethanol for 20 min at 65°C prior to reprobing. The MCID image analysis system (Imaging Research, INC., St. Catherines, Canada) was used to quantify band intensities by densitometry as previously described [22].

Two-dimensional Gel Electrophoresis

Isoelectric focusing on pI 4-7 11 cm and 17 cm strips or narrow range 4.7-5.9 11 cm strips and two-dimensional (2D) gel electrophoresis was performed as described previously [3]. The 2D gels were stained for protein using Sypro Ruby total protein stain (Invitrogen, Grand Island, NY) [3] or transferred onto PVDF membrane to detect protein succination by western blotting.

Protein Identification by Mass Spectrometry

Maldi-Tof—Spots of interest on Sypro Ruby stained gels were identified on a UV transilluminator and excised after confirming location from duplicate gels which protein succination was detected after blotting. The excised spots were processed for analysis by washing the gel pieces twice in 25 mM ammonium bicarbonate in 5% acetonitrile, followed by dehydration with 100% acetonitrile [2]. Trypsin digestion was carried out overnight at 37°C in the presence of 1.5 ng sequence grade modified trypsin in 25 mM ammonium bicarbonate. The samples were desalted on C18 Zip-Tips (Millipore, MA) and peptides were eluted with 1.5 μl of 5 mg/ml α-cyano 4-hydroxycinnaminic acid in 50% acetonitrile/0.1 % TFA directly onto a MALDI plate insert. The peptides were analyzed on a Bruker Daltonics Ultraflex MALDI TOF-TOF (Bremen, Germany) as described [6]. Protein identification was performed using Mascot software (Matrix Science, London, UK).

Lc-Ms/Ms—Tubulin bands were excised from gels after staining with Coomassie Brilliant Blue. The gel bands were washed and the protein was digested with trypsin as described above. After desalting and recovery of the peptides on C18 Zip-Tips, the samples were analyzed by LC-MS/MS on a Waters Quadrupole-Time of Flight API US. Peptides were separated by nano LC on an Agilent 1100 NanoLC pump at a flow rate of 500 nl/min. The column was a Zorbax 300SB-C18, 3.5 μm particles (150 mm × 100 μm ID). Solvent A consisted of 95% water/5% acetonitrile with 0.1% formic acid and Solvent B contained 100% acetonitrile with 0.1 % formic acid. The mobile phase gradient started at 10 % B held for 10 minutes and then ramped to 50% B over 50 min. The gradient was then ramped to 80% B over the next 30 min. MassLynx software was used to generate peak list files (pkl) which were submitted to Mascot (http://www.matrixscience.com, Matrix Science, London, UK) for protein identification from the MS/MS data.

Identification of Succinated Cysteines in Tubulin by LC-MS/MS

The excised gel bands containing purified porcine tubulin which had been incubated in 0, 0.1, 0.5, 1, 5 or 50 mM fumarate or in 500 μM DMF for 24 h at 37°C were processed for MS after washing as described above. The protein was reduced with 10 mM dithiothreitol and alkylated with 170 mM 4-vinylpyridine followed by digestion in 50 mM ammonium bicarbonate buffer containing 2 pmol of Promega sequencing grade modified trypsin (Promega, Madison, WI). The digested samples were analyzed on a Dionex Ultimate 3000-LC system (Thermo Scientific, Rockford, IL) coupled to a Velos Pro Orbitrap mass spectrometer (Thermo Scientific, Rockford, IL). A 75-μm C18 stationary-phase LC column was used with a 60 min gradient from 2% acetonitrile in 0.1% formic acid (solvent A) to 70% solvent A and 30% solvent B (60% acetonitrile containing 0.1% formic acid). The Orbitrap was operated in data-dependent MS/MS analysis mode and excluded all ions below 200 counts. An inclusion list was used to monitor select pyridylethylated and succinated tryptic peptide masses of interest for CID-MS/MS analysis. The data-dependent and CID-MS/MS data were analyzed in Proteome Discover 1.4 Software and sequenced manually using Xcalibur 2.2 Software to confirm the modified peptides. The variable modifications of methionine oxidation (M^{ox}), cysteine pyridylethylation (C^{PE}, 105.058), cysteine succination (C^{2SC}) by fumarate (116.011) or DMF (144.042) were considered. The combined charged states observed for succinated peptides were normalized to a robust internal standard peptide

(YLTVAAVFR, $[M+2H]^{2+}$ 520.2993) to determine the relative abundance of the succinated peptides.

Quantification of 2SC by Gas Chromatography - Mass Spectrometry (GC-MS/MS)

The procedure was adapted from previously described methods with minor modifications [1, 2]. Purified porcine brain tubulin (Cytoskeleton, Inc., Denver, CO) was resuspended in 0.2 M phosphate buffer, pH 7.4, containing 100 μM DTPA. Duplicate samples (500 μg tubulin) were incubated for 24 h at 37°C in the presence of either 50 mM fumarate or 500 μM DMF. Tubulin was precipitated by addition of an equal volume of cold 20% trichloroacetic acid, followed by centrifugation at 1,000 x *g* for 10 min at 4°C. Pellets were hydrolyzed in 6M HCl containing 0.5 nmol $^{13}C_3$,^{15}N-2SC, and 100 nmol d_8-lysine internal standards for 16 h at 110°C. The dried sample was resuspended in 1 ml 1% trifluoroacetic acid (TFA) and applied to a C-18 Sep-Pak column (Waters, MA) before elution with 1% TFA/20% methanol. The eluate was dried *in vacuo* and the residual amino acids were converted to their *N*,*O*-trifluoroacetyl methyl ester (TFAME) derivatives for GS/MS analysis as previously described [1, 2]. Quantification was performed by isotope-dilution mass spectrometry based on standard curves.

In Vitro Polymerization of Porcine Brain Tubulin

The effects of different concentrations of fumarate or DMF on tubulin polymerization were assessed by an adaptation of the method described by Bonne *et al.* [23], which measures the increase in fluorescence of 4′,6-diamidino-2-phenylindole (DAPI) when incorporated into polymerizing tubulin. Purified porcine brain tubulin (Cytoskeleton, Inc., Denver, CO) was dissolved in 80 mM Pipes, pH 6.9 containing 0.5 mM EGTA, and incubated with 500 μM, 1 mM, 5 mM or 50 mM fumarate, or 100 μM, 500 μM or 1 mM DMF for 6 or 24 h at room temperature in black 96 well, half area plates. Plates were incubated on ice for 10 min and polymerization initiated by addition of 80 mM Pipes, pH 6.9, containing 2 mM $MgCl_2$, 15% glycerol, 1 mM GTP and 15 μM DAPI with mixing and incubation at 37°C in a plate reader (Tecan Safire^2, TECAN Systems Inc., San Jose, CA). Kinetic measurements were performed (1 per minute for 2 h, at 350 nm excitation/430 nm emission). For data display, each individual measurement was separated into 10 min intervals that were averaged to obtain a single value for that period (Figure 4). In addition, the readings at t= 90 min were used to compare the effects of the compounds versus untreated tubulin. For the experiments designed to test the effects of microtubule associated proteins (MAPs; Cytoskeleton, Inc., Denver, CO) on tubulin polymerization, the ratio of tubulin to MAPs was 97:3 (w/w), and the concentration of glycerol was reduced to 5% to avoid disturbances of the tubulin-MAPs interactions. Further analysis of free sulfhydryl groups, western blotting and mass spectrometry in the samples was performed as described below.

Purification and Polymerization of Mouse Brain Tubulin

In vitro polymerization of mouse brain tubulin was performed according to a previously described protocol, with minor modifications [24]. Briefly, frozen whole brains from control mice (see Mouse Tissue Preparation) were reduced to a powder with a pestle in a mortar containing liquid nitrogen. The pulverized brains were then resuspended in cold Mes/

glutamate buffer (0.1 M Mes, pH 6.8, containing 0.5 mM $MgCl_2$, 1 mM EGTA, 1 M glutamate, 1 mM DTT and a protease inhibitor cocktail), in a volume ratio of 1:1.5 (powder:buffer). The suspension was pulse sonicated at 2 watts using a Model 100 sonic dismembrator (Fisher Scientific, Fair Lawn, NJ) for 5 intervals of 10 s. The total protein homogenate (H) was then centrifuged at 30,000 x *g* at 4°C for 15 min to remove cell debris (first pellet, P), and the supernatant (S) was subjected to polymerization by addition of 20 μM taxol and 1 mM GTP, followed by incubation for 30 min at 37°C. Following further centrifugation at 30,000 x *g* for 30 min at 37°C, the supernatant (SM) was removed, and the microtubular pellet was washed by resuspension with Mes/glutamate buffer containing 0.35M NaCl and 20 μM taxol, to remove loosely bound proteins. A purified microtubular pellet (M) was obtained by centrifugation at 30,000 x *g* for 30 min at 37°C. Both P and M fractions were resuspended in a mix of 50% RIPA buffer/50% PBS. All the fractions were kept at -70°C until use. Protein loading from each fraction for SDS-PAGE was performed on a volume basis using the equivalent of 3 μg protein from the initial H fraction.

Determination of Free Sulfhydryl Groups in Tubulin after Polymerization

Free sulfhydryl content was determined according to the 5,5′-dithiobis(2-nitrobenzoic acid) (DTNB) method, as described by Aitken and Learmonth [25]. The samples (see *In Vitro* Polymerization of Brain Porcine Tubulin) were diluted in 6 M guanidinium chloride prepared in 0.1 M phosphate buffer, pH 8.0, then added in triplicates to a 96-well plate (25 μg tubulin/well) and an initial reading at 412 nm was taken in a plate reader (Tecan Safire^2, TECAN Systems Inc., San Jose, CA). DTNB solution was added to the wells (0.25 mg/ml), the plate was mixed and incubated for 30 min at room temperature and a final reading was taken. Calculations were made subtracting the initial reading from the final reading, correcting with the blank, and considering E_{412} = 14150 $cm^{-1}M^{-1}$ and a path length of 0.5 cm.

Cell Proliferation Assay

Cell proliferation of 3T3-L1 fibroblasts was assessed after treatment with different concentrations of DMF, using a CyQUANT® Cell Proliferation Assay Kit (Invitrogen, Grand Island, NY). Cells were plated in 24-wells plates at a density of 10,000 cells per well, and allowed to attach and proliferate for 24 h. 10 μM, 50 μM, 100 μM, or 500 μM DMF prepared in fresh DMEM was added to treatment wells. After an additional 24 h incubation period, cells were observed under the microscope for gross morphological changes, media was removed, and cells were gently rinsed with PBS and then frozen and kept at -70°C until assay. To assess cellular proliferation the DNA content was measured using the CyQUANT® Cell Proliferation Assay (Invitrogen) according to manufacturer's instructions. Values were converted to μg of DNA based on the standard curve obtained.

Statistical Analysis

Data are summarized throughout as mean ± standard error and are plotted using SigmaPlot 11 software (Systat Software, Inc. San Jose, CA) and Prism 4 (GraphPad Software, La Jolla, CA). Statistical analyses were performed using SigmaPlot 11 and Prism 4. Differences

between groups were analyzed using one way ANOVA with the Student-Newman-Keuls post-test.

Results

We have previously detected a significant increase in succination on a protein of ∼ 50 kDa both in adipocytes grown in high glucose/high insulin medium and in the adipose tissue of type 2 diabetic mice [2-5]. However, this increase in succination was not observed in skeletal muscle of type 2 diabetic mice [5]. To confirm and extend our previous results, we examined protein succination in 3T3-L1 adipocytes and in C2C12 myotubes cultured in both normal and high glucose concentrations. The anti-2SC antibody detected multiple bands in all lanes (Figure 1A), with significant increases only in the adipocytes cultured in high glucose at both 4 and 8 days. A prominent band of ∼50 kDa showed increases in 2SC content when the cells were cultured in 30 mM glucose (Figure 1A, lanes 3 and 4 vs. 1 and 2 for 4 days; lanes 7 and 8 vs. 5 and 6 for 8 days). In contrast, the intensity of the ∼50 kDa band in C2C12 myotubes did not increase in 25 mM vs. 5 mM glucose (Figure 1A, lanes 11 and 12 vs. lanes 9 and 10). The blot was stripped and reprobed with an anti-actin antibody; notably the actin content was higher in C2C12 myotubes (∼42 kDa, Figure 1B, lanes 9-12 vs. lanes 1-8). The blot was also reprobed with an anti-β-tubulin antibody, yielding a band at ∼50 kDa that corresponded to the molecular weight of the prominent 2SC band (Figure 1C). Coomassie staining of the blot (Figure 1D) indicated that actin (∼42 kDa) is more abundant than other proteins, especially in the C2C12 myotubes, suggesting that the accumulation of the 2SC modification is not related to protein abundance but is instead specific to certain proteins with reactive thiols.

2D-PAGE separation was employed to further study the succinated ∼50 kDa region in C2C12 cells cultured in 25 mM glucose. The anti-2SC antibody detected a series of spots resolved at ∼50 kDa, with isoelectric points ranging ∼ 4.5 - 5.0 (Figure 2A). The Coomassie staining of the blot (Figure 2B) showed several proteins and confirmed that the heavily succinated protein (Figure 2A, ∼50 kDa) was not the most abundant protein (Figure 2B, ∼42 kDa). After spot picking from a duplicate gel stained with Sypro Ruby (Figure 2C) the succinated protein spots at ∼50 kDa were identified as β-tubulin by MALDI-TOF mass spectrometry (Table 1). To confirm this data, C2C12 cells extracts were immunoprecipitated with an anti-β-tubulin antibody and immunoblotted with anti-2SC antibody. The immunoprecipitated tubulin reacted strongly with the 2SC antibody (Figure 2D, middle panel) and this band was also reactive for β-tubulin (actual MW 55 kDa, Figure 2D, third panel). The most abundant Coomassie spots in the C2C12 cells (∼42 kDa, Figure 2B) were confirmed to be actin by mass spectrometry (data not shown).

2D-PAGE analysis was also used to resolve the ∼50 kDa region in 3T3 adipocytes grown in 30 mM glucose. In agreement with the 1D blot (Figure 1A) protein succination was increased on several proteins, corresponding to a larger number of succinated spots (Figure 3A). Figure 3B focuses on a region of Figure 3A (boxed) containing proteins ∼50 kDa and the isoelectric points 4.4 to 5.0. The upper 2SC panel highlights the major succinated proteins and these were matched to several Sypro Ruby spots in a duplicate gel (solid and dashed circles). Reprobing the blot with antibodies against α- and β-tubulin and matching

with the 2SC blot suggested that both α-tubulin (dashed circle) and β-tubulin (solid circle) were the succinated proteins (Figure 3B, lower panels). This was confirmed after excision of the spots and identification of several α- and β-tubulin isoforms by LC-MS/MS (Table 2). The other abundant succinated spot on the far left (*, 2SC panel, Figure 3B) was confirmed to be Protein Disulfide Isomerase (data not shown) and is the subject of other investigations in our laboratory. As with the C2C12 cells, immunoprecipitation of β-tubulin from 3T3 cell lysates and subsequent 2SC probing confirmed that β-tubulin was succinated (Figure 3C). To extend these observations to the adipose tissue of diabetic mice, we used mesenteric fat extracts from *db/db* mice. As shown in Figure 3D and E, 2D-PAGE separation (pI 4.7-5.9) of immunoprecipitated β-tubulin confirmed its succination in the adipose tissue of the diabetic *db/db* mouse.

Considering that tubulin isoforms are targets of succination both *in vitro* and *in vivo*, we proposed that succination may affect tubulin polymerization. To test this hypothesis, we examined the *in vitro* polymerization of purified porcine brain tubulin (as tubulin is an abundant protein in the brain and purified porcine tubulin is readily available). Porcine tubulin was incubated with different concentrations of fumarate or the more reactive fumarate ester, dimethylfumarate (DMF). As shown in Figure 4A, preincubation of tubulin with fumarate for 24 h (range of concentrations: 500 μM to 50 mM) lowered tubulin polymerization in statistically significant manner at 50 mM (35% decrease, $p<0.05$, n=3, Figure 4B); decreased polymerization at 5 mM fumarate was also observed, although this did not reach statistical significance (Figure 4B). The preincubation of tubulin with DMF for 6 h (100 μM - 1 mM) reduced tubulin polymerization (Figure 4C), with significant reductions at 500 μM and 1 mM. Incubation of tubulin with 500 μM DMF for 24 h inhibited tubulin polymerization by 59% (Figures 4A and 4B, $p<0.001$). Incubation for 24 h with 500 μM 4-hydroxynonenal prevented tubulin polymerization in a similar manner to DMF treatment (positive control, data not shown). Microtubule associated proteins (MAPs) are known to favor the incorporation of tubulin dimers into microtubules, as they are basic proteins able to interact with the negatively charged C-terminal tails of tubulin (CTT) [26]. As succination in the presence of 50 mM fumarate decreased tubulin polymerization by increasing the negative charge of tubulin, we hypothesized that the additional presence of MAPs might overcome this effect. A global positive effect of MAPs on tubulin polymerization was observed (Figure 4D, $p<0.001$ for No MAPs vs. MAPs comparison); furthermore, MAPs enhanced tubulin polymerization of succinated tubulin to levels that were approximately equal to control tubulin (Figure 4D, NS for control + MAPs vs. 50 mM fumarate + MAPs). This was in clear contrast with tubulin subjected to polymerization in the absence of MAPs (Figure 4D, $p<0.01$ for control vs. 50 mM fumarate).

We also analyzed the 2SC content of porcine brain tubulin by GC-MS/MS after incubation with 50 mM fumarate or 500 μM DMF for 24 h at 37°C. As shown in Table 3, the levels of 2SC (mmol/mol Lys) increase ∼47-fold in the presence of 50 mM fumarate, and ∼2000-fold when incubated with 500 μM DMF. The DTNB assay was used to quantify the number of free sulfhydryl groups in porcine brain tubulin after modification by fumarate or DMF. Of the 20 –SH groups in the tubulin dimer ∼12 were detected and incubation with fumarate (500 μM to 50 mM) did not result in a detectable loss of these thiol groups (Figure 4E).

However, incubation of tubulin in DMF resulted in ∼25% reduction in thiol content at 500 μM and 1 mM concentrations ($p<0.05$, Figure 4E). Proteomic analysis of tubulin modification by DMF revealed that 11 of the 20 total cysteines in the dimer were succinated; including Cys 295, 315, 316, 347 and 376 in α-tubulin and Cys 12, 127, 129, 239, 303 and 354 in β-tubulin (Table 4).

Our anti-2SC antibody indicates that mouse brain tubulin has a significant level of basal endogenous succination. We investigated if this basal succination of tubulin present in normal mouse brain extracts could alter its ability to polymerize in the presence of taxol. Figure 4F shows that most of the succinated tubulin (upper panel), α-tubulin (middle panel) and β-tubulin (lower panel) initially present in the total protein homogenate (H) appeared in the first supernatant (S) as unpolymerized tubulin, with only a small polymerized fraction present in the pellet (P) after centrifugation. When S was subjected to polymerization in the presence of taxol, the majority of succinated α- and β-tubulin was pulled down into the microtubular pellet (M), as no immunoreactive bands were detected in the supernatant after polymerization (SM). These results indicate that endogenous levels of tubulin succination do not interfere with tubulin polymerization in the presence of taxol. Considering that many tubulin modifications including acetylation are present on stable, long-lived axons [7], we initially hypothesized that succinated tubulin would be present at higher levels in stable microtubules *in vivo.* To test this, we examined protein homogenates from control mouse brain (containing less stable microtubules from neuronal bodies) vs. sciatic nerve (more stable microtubules from axons). Increasing amounts of sciatic nerve protein (10-40 μg) were compared with 10 μg of brain protein. We observed that 20μg of sciatic nerve homogenate was equivalent to 10 μg of brain homogenate in the total tubulin content (Figure 4G, α-tubulin, β-tubulin and Coomassie panels). Succination was abundant in 10 μg of brain homogenate when compared to an equivalent (or greater) amount of tubulin in the sciatic nerve (Figure 4G, 2SC panel), indicating that succination is more prominent in the more dynamic microtubules of the brain than in stable microtubules from axons of the sciatic nerve.

Purified porcine brain tubulin which had been incubated with fumarate and subjected to polymerization (Figure 4B) was next separated by PAGE. Increased succination was evident for 0.5-50 mM fumarate treated samples vs. unmodified control tubulin (2SC panel, Figure 5A). Notably, reprobing this blot with anti-α-tubulin B-7 demonstrated a loss of immunoreactivity at high fumarate concentrations; however, a Coomassie stain of total protein content demonstrated equal protein loading (α-tubulin and Coomassie panels, Figure 5A). Densitometric analysis of the bands indicated that the reduction in α-tubulin immunoreactivity was significant at 1, 5 and 50 mM fumarate ($p<0.05$, $p<0.001$ and $p<0.001$ vs. untreated control, respectively, Figure 5B). This strongly suggested that increased modification by fumarate prevented binding of this α- tubulin antibody. In addition, reprobing with anti-β-tubulin TUB2.1 also indicated some reduction in immunoreactivity, which was significant at 5 and 50 mM fumarate ($p<0.001$ vs. untreated control; β-tubulin vs. Coomassie panel, Figure 5A and Figure 5B). The anti-2SC antibody does not recognize the DMF succinated moiety without prior removal of the ester group [27]; therefore these samples were not analyzed by western immunoblotting. Non-confluent

3T3 fibroblasts were incubated in 5 mM glucose with an addition of 10 – 500 μM DMF for 24 h. The DNA content of the proliferating cells was significantly reduced in 50, 100 and 500 μM DMF ($p<0.001$, Figure 5C). Figure 5D (upper panel, 2SC) shows that 24 h incubation with 50 mM fumarate increased the content of several succinated proteins in 3T3 fibroblasts, including a ∼50 kDa band (dashed line). When the same blot was reprobed with anti α-tubulin B-7, the intensity of the band decreased, confirming the *in vitro* results with purified brain tubulin (Figure 5A and B). We again examined tubulin succination and α- and β-tubulin levels in the 30 mM vs. 5 mM glucose treated adipocytes after 8 days. As shown in Figure 5E, incubation of adipocytes in 30 mM glucose increased succination of the ∼50 kDa band and at the same time decreased the B-7 antibody detection of α-tubulin; however Coomassie staining of the blot showed equal loading. Quantification of the bands showed a significant decrease of the α-tubulin band ($p<0.01$, Figure 5F), again suggesting that succination of tubulin blocks the binding capacity of this anti-α-tubulin antibody.

We used high resolution mass spectrometry to identify the sites of succination in the porcine brain tubulin samples that were incubated with increasing concentrations of fumarate (see previous Figure 4A and B, Figure 5A). Cys12 was the primary site of succination in β-tubulin (sequencing of tryptic peptide containing Cys12β in 5mM fumarate is shown, Figure 6B). Unmodified cysteines were detected as pyridylethylated cysteines in control unmodified tubulin (Figure 6 A and C). A relative increase in succination at Cys 12β and also at Cys 303β was detected in 1 mM, 5 mM and 50 mM fumarate (Figure 6E). We also identified Cys347α as a prominent site of succination in α-tubulin (Figure 6D), and increased levels of 2SC were detected in 1, 5 and 50 mM vs. unmodified control tubulin (Figure 6F). Cys376 of α-tubulin was also succinated; however this was only detected in the 50 mM fumarate incubation (Figure 6F).

Finally, after identifying the primary sites of succination in both α- and β-tubulin, we re-evaluated the change in immunodetectability of succinated tubulin with antibodies targeting different sequences in the structure of both subunits. Figure 7 confirms that the B-7 antibody again detected lower amounts of α-tubulin when the protein was incubated with 50 mM fumarate compared to control tubulin; according to the manufacturer this antibody was raised using a peptide that contained both Cys347α and Cys376α. However, the decrease in immunoreactivity is barely observed for DM1A, an antibody that targets a region surrounding Val 440α (Figure 7). Regarding β-tubulin, we again observed a decrease in the detectability of succinated tubulin by TUB2.1 (Figure 7); the antigen for this antibody is in a region containing Cys303β [28]. In contrast, no change in detection of succinated β-tubulin was observed when D65A4 was used, consistent with the manufacturer's confirmation that the antibody was not raised against regions containing either Cys12β or Cys303β (Figure 7). In addition, the less specific polyclonal antibody ATN02, designed to target multiple epitopes in both α- and β-tubulin, was unable to detect changes in tubulin immunoreactivity according to the succination state of the protein (Figure 7).

Discussion

We have previously described an increase in protein succination in adipocytes grown in high glucose medium and have confirmed the identity of ∼40 of these proteins [2, 29]. In the

current study, we identified a prominent succinated protein ∼50 kDa that is increased in adipocytes during exposure to high glucose medium (Figure 1A) and in the adipose tissue of type 2 diabetic mice [2, 5]. This succinated band was also prominent in mouse skeletal muscle, heart, testes and lungs [5] and in C2C12 myotubes (Figure 1A), but the level of endogenous succination did not change in these tissues during diabetes [5]. This suggests that the metabolic characteristics of different cell types have a role in the degree of protein succination [4]. The limited succination in the C2C12 myotubes provided a useful model to further investigate the nature of the succinated ∼50 kDa protein. We now confirm the identification of this protein in myotubes (Table 1, Figure 2D) and adipocytes (Table 2, Figures 3C-E) as both α- and β-tubulins, adding this novel modification to the other documented PTMs of the αβ tubulin dimer. In addition, we confirm that tubulin succination is an abundant modification in the healthy (control) brain (Figure 4G), in part due to the abundance of tubulin in the brain, but notably it was not as prominent in the axonal microtubules axons of the sciatic nerve (Figure 4G). These are generally considered to be more stable microtubules than those found in neuronal cell bodies [30, 31] and suggests there is some selectivity in the microtubule regions that are most succinated. Selective succination of more dynamic tubulins may be linked to the role of this modification in the central nervous system.

Tubulin succination appears to be a specific event as succination is not necessarily targeted to the most abundant proteins in the samples. In fact, actin (∼42 kDa) is more prominent than tubulin (∼50 kDa) in the myotubes compared to adipocytes (Figure 1B and 1D) and it has free thiols, yet succination is clearly more abundant on tubulin in these samples (Figures 1 and 2). In other work [29, 32] we have described that fumarate most likely reacts with low pK_a thiols, and that their reactivity will also be affected by their accessibility on the protein. The reactivity of some tubulin thiols towards various sulfhydryl agents has previously been examined [16, 17, 20] and many of the documented sites of succination are similar to those we have identified in this study (Figure 6, Table 4), confirming that exposed or low pK_a thiols are most reactive with fumarate. Protein modification by fumarate generates a stable thioether adduct which, like the 4-HNE modification, is likely enzymatically irreversible and cumulative with the life of the protein.

Fumarate had a limited but significant effect on reducing tubulin polymerization *in vitro* and it will be important to determine if lower fumarate concentrations altered microtubule length when succinated tubulin is incorporated into microtubules in future studies. Other electrophilic reagents have been previously used to modify the cysteine residues of tubulin. For example, iodoacetamide (50:1 molar ratio to tubulin) blocked 10 out of 20 –SH groups of the tubulin dimer; however no effect on polymerization was described in this report [20]. In addition, N-ethylmaleimide (NEM), another electrophilic agent that reacts with cysteine residues generating an uncharged product, was also used to target –SH groups of tubulin [17]. At 1:1 and 4:1 ratios to tubulin, NEM blocked tubulin polymerization by 71% and 100%, respectively. In that same study, MAPs only partially abolished NEM effect on tubulin polymerization (at NEM to tubulin 1:1 ratio), or had no effect (at NEM to tubulin 4:1 ratio). When we used the much less reactive electrophile fumarate at 50 mM, we observed a 35% decrease in tubulin polymerization that was abolished in the presence of MAPs,

confirming that fumarate is less reactive than iodoacetamide and NEM, however, it is a physiologically relevant endogenous electrophile that is clearly capable of basal succination *in vivo*. The increase in succination observed in certain (patho)physiological states (adipocyte in diabetes) may alter tubulin polymerization in vivo. In contrast, our study showed that 500 μM dimethylfumarate (DMF), effectively reduced tubulin polymerization by 59%, demonstrating the stronger reactivity of the fumarate ester with cysteine residues compared to fumarate.

It is remarkable that *in vitro* succination decreased the affinity of the anti α-tubulin B-7 (and to a lesser degree the anti β-tubulin TUB2.1) antibodies for the protein (Figure 5A and B), while it did not affect the ability of other antibodies to detect tubulin (Figure 7). The ability of succination to interfere with antibody recognition of specific epitopes suggests that succination of certain cysteines may significantly affect the ability of tubulin to associate with other proteins. While our polymerization assays using fumarate-treated tubulin in the presence of MAPs (Figure 4D) indicate that the interactions of tubulin with MAP1/2 and Tau are unaltered by succination, we cannot rule out a possible disruption of tubulin association with other proteins, including molecular motors as dynein and kinesin. Considering that the C-terminal tail is essential for MAP1/2 interaction then it is conceivable that succination may not alter the interaction of these proteins. Other tubulin post-translational modifications including acetylation, tyrosination and polyglutamylation have been associated with increases in both microtubule stability and microtubule affinity for the molecular motors dynein and kinesin [33, 34]. Many of these modifications are found on the CTT and have been proposed to form a ‘tubulin code’ that may alter the trafficking of cargo along microtubules [34], however, the kinesins and dynein can still associate with tubulin and move along the microtubule even in the absence of the CTT [34], suggesting that interactions with other regions of tubulin also have a role. The α-tubulin monoclonal antibody B-7 that we used initially was raised against amino acids 149-448 of α-tubulin of human origin, a portion of the protein which contains 8 cysteine residues, including several residues that have been documented to react rapidly with other thiol modifying agents (Cys305, Cys315, Cys316, Cys347, and Cys376) [20]. We identified succinated Cys347α in 1, 5 and 50 mM fumarate incubations, concentrations that all demonstrated significant reductions in anti-α-tubulin recognition, and succinated Cys376α in 50 mM fumarate (Figure 6). Cys347α has been documented to be the most reactive exposed cysteine [20] and is also the primary target for tubulin modification by isothiocyanates [35], which may explain the reduced antibody immunoreactivity. Our results strongly suggest that Cys347α forms part of the epitope recognized by this α-tubulin antibody and in future work it will be important to determine if succination at this site alters interactions between tubulin and other proteins. Succination of Cys376α was only observed at 50 mM fumarate, however, this cysteine is nearly buried but is documented to be modified by palmitoylation [36, 37]. The maximum fumarate concentration endogenously produced is ∼5 mM as detected in fumarate hydratase deficient fibroblasts in which succination of proteins is significantly increased [38]. Therefore, our data indicating significant modification at both 1 and 5 mM fumarate (Figure 6) has important physiological implications as we have previously shown that fumarate levels increase up to 5-fold in adipocytes exposed to 30 mM (high) glucose vs. 5 mM glucose [2], and anti-α-tubulin immunoreactivity was also reduced in these 30 mM

glucose treated adipocytes (Figure 5 E and F). Overall, the observation that tubulin:antibody interactions are altered as a result of succination, combined with the evidence that succination is predominant on dynamic versus axonal microtubules has important implications for the role of this modification in intracellular organelle trafficking.

In addition to α-tubulin, we also observed that succination was increased on Cys12 and Cys303 of β-tubulin (Figure 6). Cys12β is involved in GTP binding, as indicated by photoaffinity labeling experiments [39]. Our finding that Cys12β is succinated when fumarate levels are elevated raises the interesting possibility that succination could affect GTP binding and thus interfere with the normal microtubule dynamics, as recently shown for the natural product derivative bis(4-fluorobenzyl)trisulfide that also binds to Cys-12β [40].

In the present study, we also used the reactive fumarate ester DMF as an alternative to assess the effects of succination on tubulin polymerization. This compound was approved in the US in 2013 for the treatment of multiple sclerosis after proving beneficial in clinical trials [41]. To date, the primary mechanism of action for DMF has been proposed to be linked to the activation of the transcription factor Nrf2 via modification of Keap 1, consequently increasing the intracellular antioxidant response [42]. In addition, DMF has been demonstrated to react rapidly with intracellular glutathione pools, requiring the cell to produce more glutathione as part of the antioxidant response [43-45]. Our novel data demonstrates for the first time that DMF, at concentrations similar to those currently prescribed in oral medications [46, 47], also reacts specifically with cysteine residues on tubulin reducing its ability to polymerize (Figure 4C). We specifically demonstrated by proteomic analysis that as many as 11 of the 20 cysteines in αβ -tubulin were succinated by DMF (Table 4), including the documented sites modified by fumarate (Figure 6). In addition, micromolar treatment of proliferating fibroblasts with DMF significantly lowers the DNA content of these cells (Figure 5C). We propose that inhibition of tubulin polymerization by DMF may be a novel and important alternative mechanism of action that contributes to reduced inflammatory cell proliferation after fumarate ester treatment. Gastrointestinal (GI) discomfort is the most common side effect of DMF treatment resulting in discontinued use for some patients. Our results suggest that, similar to the anti-proliferative effects of chemotherapeutic agents on the GI tract, DMF may inhibit cellular proliferation by interfering with microtubule dynamics; providing an explanation for the GI discomfort and warranting further studies on its effects on fetal growth during pregnancy [48]. Several other recent reports suggest a putative anti-proliferative effect of fumarate esters [49-51] and an anti-angiogenic effect has also been described in endothelial cells [52]. Our data suggests that this could be attributed in part to the inhibitory actions of this drug on tubulin polymerization.

In conclusion, we demonstrate that succination is a novel tubulin modification and propose that endogenous increases in fumarate levels may alter the interaction of tubulin with other proteins. We also show that reactive alkylfumarates may limit microtubule dynamics by inhibiting polymerization; defining an alternative mechanism of action for these compounds and highlighting their potential utility as anti-cancer therapeutics.

Acknowledgments

We thank Professor John W Baynes, USC and Dr. Deanna Smith, USC for helpful discussion.

Funding: This work was supported by grants from the National Institute of Diabetes & Digestive & Kidney Diseases (DK-19971), the American Diabetes Association (1-11-JF-13) and a University of South Carolina Research Foundation ASPIRE-1 award.

References

1. Alderson NL, Wang Y, Blatnik M, Frizzell N, Walla MD, Lyons TJ, Alt N, Carson JA, Nagai R, Thorpe SR, Baynes JW. S-(2-Succinyl)cysteine: a novel chemical modification of tissue proteins by a Krebs cycle intermediate. Arch Biochem Biophys. 2006; 450:1–8. [PubMed: 16624247]
2. Nagai R, Brock JW, Blatnik M, Baatz JE, Bethard J, Walla MD, Thorpe SR, Baynes JW, Frizzell N. Succination of protein thiols during adipocyte maturation: a biomarker of mitochondrial stress. J Biol Chem. 2007; 282:34219–34228. [PubMed: 17726021]
3. Frizzell N, Rajesh M, Jepson MJ, Nagai R, Carson JA, Thorpe SR, Baynes JW. Succination of thiol groups in adipose tissue proteins in diabetes: succination inhibits polymerization and secretion of adiponectin. J Biol Chem. 2009; 284:25772–25781. [PubMed: 19592500]
4. Frizzell N, Thomas SA, Carson JA, Baynes JW. Mitochondrial stress causes increased succination of proteins in adipocytes in response to glucotoxicity. Biochem J. 2012; 445:247–254. [PubMed: 22524437]
5. Thomas SA, Storey KB, Baynes JW, Frizzell N. Tissue distribution of S-(2-succino)cysteine (2SC), a biomarker of mitochondrial stress in obesity and diabetes. Obesity. 2012; 20:263–269. [PubMed: 22134201]
6. Blatnik M, Frizzell N, Thorpe SR, Baynes JW. Inactivation of glyceraldehyde-3-phosphate dehydrogenase by fumarate in diabetes: formation of S-(2-succinyl)cysteine, a novel chemical modification of protein and possible biomarker of mitochondrial stress. Diabetes. 2008; 57:41–49. [PubMed: 17934141]
7. Garnham CP, Roll-Mecak A. The chemical complexity of cellular microtubules: Tubulin post-translational modification enzymes and their roles in tuning microtubule functions. Cytoskeleton. 2012; 69:442–463. [PubMed: 22422711]
8. Perdiz D, Mackeh R, Poüs C, Baillet A. The ins and outs of tubulin acetylation: more than just a post-translational modification? Cell Signal. 2011; 23:763–771. [PubMed: 20940043]
9. Janke C, Rogowski K, van Dijk J. Polyglutamylation: a fine-regulator of protein function? ‘Protein Modifications: beyond the usual suspects’ review series. EMBO Rep. 2008; 9:636–641. [PubMed: 18566597]
10. Janke C, Rogowski K, Wloga D, Regnard C, Kajava AV, Strub JM, Temurak N, van Dijk J, Boucher D, van Dorsselaer A, Suryavanshi S, Gaertig J, Eddé B. Tubulin polyglutamylase enzymes are members of the TTL domain protein family. Science. 2005; 308:1758–1762. [PubMed: 15890843]
11. Landino LM, Hasan R, McGaw A, Cooley S, Smith AW, Masselam K, Kim G. Peroxynitrite oxidation of tubulin sulfhydryls inhibits microtubule polymerization. Arch Biochem Biophys. 2002; 398:213–220. [PubMed: 11831852]
12. Landino LM, Koumas MT, Mason CE, Alston JA. Modification of tubulin cysteines by nitric oxide and nitroxyl donors alters tubulin polymerization activity. Chem Res Toxicol. 2007; 20:1693–1700. [PubMed: 17907787]
13. Dremina ES, Sharov VS, Schöneich C. Protein tyrosine nitration in rat brain is associated with raft proteins, flotillin-1 and alpha-tubulin: effect of biological aging. J Neurochem. 2005; 93:1262–1271. [PubMed: 15934946]
14. Neely MD, Sidell KR, Graham DG, Montine TJ. The lipid peroxidation product 4-hydroxynonenal inhibits neurite outgrowth, disrupts neuronal microtubules, and modifies cellular tubulin. J Neurochem. 1999; 72:2323–2333. [PubMed: 10349841]

15. Paron I, D'Elia A, D'Ambrosio C, Scaloni A, D'Aurizio F, Prescott A, Damante G, Tell G. A proteomic approach to identify early molecular targets of oxidative stress in human epithelial lens cells. Biochem J. 2004; 378:929–937. [PubMed: 14678012]
16. Chavez J, Chung WG, Miranda CL, Singhal M, Stevens JF, Maier CS. Site-specific protein adducts of 4-hydroxy-2(E)-nonenal in human THP-1 monocytic cells: protein carbonylation is diminished by ascorbic acid. Chem Res Toxicol. 2010; 23:37–47. [PubMed: 20043646]
17. Stewart BJ, Doorn JA, Petersen DR. Residue-specific adduction of tubulin by 4-hydroxynonenal and 4-oxononenal causes cross-linking and inhibits polymerization. Chem Res Toxicol. 2007; 20:1111–1119. [PubMed: 17630713]
18. Neely MD, Boutte A, Milatovic D, Montine TJ. Mechanisms of 4-hydroxynonenal-induced neuronal microtubule dysfunction. Brain Res. 2005; 1037:90–98. [PubMed: 15777756]
19. Aksenov MY, Aksenova MV, Butterfield DA, Geddes JW, Markesbery WR. Protein oxidation in the brain in Alzheimer's disease. Neuroscience. 2001; 103:373–383. [PubMed: 11246152]
20. Britto PJ, Knipling L, Wolff J. The local electrostatic environment determines cysteine reactivity of tubulin. J Biol Chem. 2002; 277:29018–29027. [PubMed: 12023292]
21. Lowry OH, Rosenbrough NJ, Farr AL, Randall RJ. Protein measurement with the Folin phenol reagent. J Biol Chem. 1951; 193:265–275. [PubMed: 14907713]
22. Piroli GG, Reznikov LR, Grillo CA, Hagar JM, Fadel JR, Reagan LP. Tianeptine modulates amygdalar glutamate neurochemistry and synaptic proteins in rats subjected to repeated stress. Exp Neurol. 2013; 241:184–193. [PubMed: 23262120]
23. Bonne D, Heusele C, Simon C, Pantaloni D. 4′,6-Diamidino-2-phenylindole, a fluorescent probe for tubulin and microtubules. J Biol Chem. 1985; 260:2819–2825. [PubMed: 3972806]
24. Miller LM, Xiao H, Burd B, Horwitz SB, Angeletti RH, Verdier-Pinard P. Methods in tubulin proteomics. Methods Cell Biol. 2010; 95:105–126. [PubMed: 20466132]
25. Aitken, A.; Learmonth, M. Estimation of disulfide bonds using Ellman's reagent. In: Walker, JM., editor. The Protein Protocols Handbook. 2nd. Humana Press; Totowa, New Jersey: 2002. p. 595-596.
26. Sackett DL, Bhattacharyya B, Wolff J. Promotion of tubulin assembly by carboxyterminal charge reduction. Ann N Y Acad Sci. 1986; 466:460–466. [PubMed: 3460425]
27. Manuel AM, Frizzell N. Adipocyte protein modification by Krebs cycle intermediates and fumarate ester derived succination. Amino Acids. 2013; 45:1243–1247. [PubMed: 23892396]
28. Matthes T, Wolff A, Soubiran F, Gros F, Dighiero G. Antitubulin antibodies. II. Natural autoantibodies and induced antibodies recognize different epitopes on the tubulin molecule. J Immunol. 1988; 141:3135–3141. [PubMed: 2459243]
29. Merkley ED, Metz TO, Smith RD, Baynes JW, Frizzell N. The succinated proteome. Mass Spectrom Rev. 2014; 33:98–109. [PubMed: 24115015]
30. Brady ST, Tytell M, Lasek RJ. Axonal tubulin and axonal microtubules: Biochemical evidence for cold stability. J Cell Biol. 1984; 99:1716–1724. [PubMed: 6490717]
31. Binet S, Meininger V. Biochemical basis of microtubule cold stability in the peripheral and central nervous systems. Brain Res. 1988; 450:231–236. [PubMed: 3401712]
32. Frizzell N, Lima M, Baynes JW. Succination of proteins in diabetes. Free Radic Res. 2011; 45:101–109. [PubMed: 20964553]
33. Janke C, Bulinski JC. Post-translational regulation of the microtubule cytoskeleton: mechanisms and functions. Nat Rev Mol Cell Biol. 2011; 12:773–786. [PubMed: 22086369]
34. Sirajuddin M, Rice LM, Vale RD. Regulation of microtubule motors by tubulin isotypes and post-translational modifications. Nat Cell Biol. 2014; 16:335–344. [PubMed: 24633327]
35. Xiao Z, Mi L, Chung FL, Veenstra TD. Proteomic analysis of covalent modifications of tubulins by isothiocyanates. J Nutr. 2012; 142:1377S–1381S. [PubMed: 22649267]
36. Ozols J, Caron JM. Posttranslational modification of tubulin by palmitoylation: II. Identification of sites of palmitoylation. Mol Biol Cell. 1997; 8:637–645. [PubMed: 9247644]
37. Zhao Z, Hou J, Xie Z, Deng J, Wang X, Chen D, Yang F, Gong W. Acyl-biotinyl exchange chemistry and mass spectrometry-based analysis of palmitoylation sites of in vitro palmitoylated rat brain tubulin. Protein J. 2010; 29:531–537. [PubMed: 20976533]

38. Ternette N, Yang M, Laroyia M, Kitagawa M, O'Flaherty L, Wolhulter K, Igarashi K, Saito K, Kato K, Fischer R, Berquand A, Kessler BM, Lappin T, Frizzell N, Soga T, Adam J, Pollard PJ. Inhibition of mitochondrial aconitase by succination in fumarate hydratase deficiency. Cell Rep. 2013; 3:689–700. [PubMed: 23499446]

39. Shivanna BD, Mejillano MR, Williams TD, Himes RH. Exchangeable GTP binding site of beta-tubulin. Identification of cysteine 12 as the major site of cross-linking by direct photoaffinity labeling. J Biol Chem. 1993; 268:127–132. [PubMed: 8416920]

40. Xu W, Xi B, Wu J, An H, Zhu J, Abassi Y, Feinstein SC, Gaylord M, Geng B, Yan H, Fan W, Sui M, Wang X, Xu X. Natural product derivative Bis(4-fluorobenzyl)trisulfide inhibits tumor growth by modification of beta-tubulin at Cys 12 and suppression of microtubule dynamics. Mol Cancer Ther. 2009; 8:3318–3330. [PubMed: 19996274]

41. Fox RJ, Miller DH, Phillips JT, Hutchinson M, Havrdova E, Kita M, Yang M, Raghupathi K, Novas M, Sweetser MT, Viglietta V, Dawson KT. CONFIRM Study Investigators. Placebo-controlled phase 3 study of oral BG-12 or glatiramer in multiple sclerosis. N Engl J Med. 2012; 367:1087–1097. [PubMed: 22992072]

42. Linker RA, Lee DH, Ryan S, van Dam AM, Conrad R, Bista P, Zeng W, Hronowsky X, Buko A, Chollate S, Ellrichmann G, Brück W, Dawson K, Goelz S, Wiese S, Scannevin RH, Lukashev M, Gold R. Fumaric acid esters exert neuroprotective effects in neuroinflammation via activation of the Nrf2 antioxidant pathway. Brain. 2011; 134:678–692. [PubMed: 21354971]

43. Ghoreschi K, Brück J, Kellerer C, Deng C, Peng H, Rothfuss O, Hussain RZ, Gocke AR, Respa A, Glocova I, Valtcheva N, Alexander E, Feil S, Feil R, Schulze-Osthoff K, Rupec RA, Lovett-Racke AE, Dringen R, Racke MK, Röcken M. Fumarates improve psoriasis and multiple sclerosis by inducing type II dendritic cells. J Exp Med. 2011; 208:2291–2303. [PubMed: 21987655]

44. Schmidt MM, Dringen R. Fumaric acid diesters deprive cultured primary astrocytes rapidly of glutathione. Neurochem Int. 2010; 57:460–467. [PubMed: 20096739]

45. Thiessen A, Schmidt MM, Dringen R. Fumaric acid dialkyl esters deprive cultured rat oligodendroglial cells of glutathione and upregulate the expression of heme oxygenase 1. Neurosci Lett. 2010; 475:56–60. [PubMed: 20347008]

46. Gold R, Linker RA, Stangel M. Fumaric acid and its esters: an emerging treatment for multiple sclerosis with antioxidative mechanism of action. Clin Immunol. 2012; 142:44–48. [PubMed: 21414846]

47. Scannevin RH, Chollate S, Jung MY, Shackett M, Patel H, Bista P, Zeng W, Ryan S, Yamamoto M, Lukashev M, Rhodes KJ. Fumarates promote cytoprotection of central nervous system cells against oxidative stress via the nuclear factor (erythroid-derived 2)-like 2 pathway. J Pharmacol Exp Ther. 2012; 341:274–284. [PubMed: 22267202]

48. Linker RA, Gold R. Dimethyl fumarate for treatment of multiple sclerosis: mechanism of action, effectiveness, and side effects. Curr Neurol Neurosci Rep. 2013; 13:394. [PubMed: 24061646]

49. Meissner M, Valesky EM, Kippenberger S, Kaufmann R. Dimethyl fumarate - only an anti-psoriatic medication? J Dtsch Dermatol Ges. 2012; 10:793–801. [PubMed: 22897153]

50. Valero T, Steele S, Neumüller K, Bracher A, Niederleithner H, Pehamberger H, Petzelbauer P, Loewe R. Combination of dacarbazine and dimethylfumarate efficiently reduces melanoma lymph node metastasis. J Invest Dermatol. 2010; 130:1087–1094. [PubMed: 19940857]

51. Yamazoe Y, Tsubaki M, Matsuoka H, Satou T, Itoh T, Kusunoki T, Kidera Y, Tanimori Y, Shoji K, Nakamura H, Ogaki M, Nishiura S, Nishida S. Dimethylfumarate inhibits tumor cell invasion and metastasis by suppressing the expression and activities of matrix metalloproteinases in melanoma cells. Cell Biol Int. 2009; 33:1087–1094. [PubMed: 19595779]

52. García-Caballero M, Marí-Beffa M, Medina MA, Quesada AR. Dimethylfumarate inhibits angiogenesis in vitro and in vivo: a possible role for its antipsoriatic effect? J Invest Dermatol. 2011; 131:1347–1355. [PubMed: 21289642]

Abbreviations Used

2SC	S-(2-succino)cysteine

DMEM	Dulbecco's modified Eagle's medium
DTPA	diethylenetriaminepentaacetic acid
FBS	fetal bovine serum
MALDI-TOF	Matrix-assisted laser desorption ionization-time of flight
PTM	post-translational modification

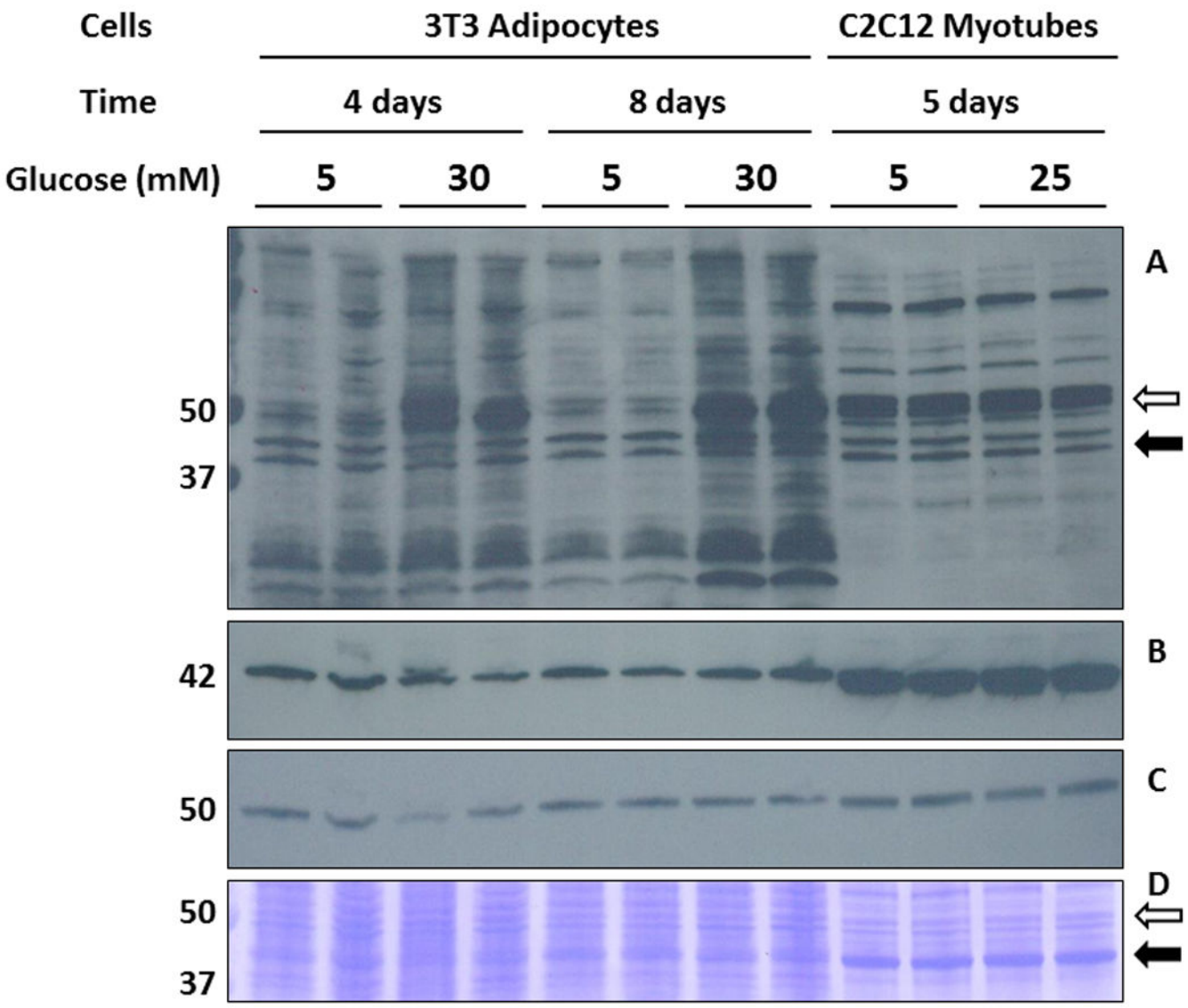

Figure 1.

High glucose medium increases succination on a ~50 kDa band in adipocytes. (A) Total cell lysates (40 μg protein) from 3T3 adipocytes matured for either 4 days in 5 mM (lanes 1-2) and 30 mM glucose (lanes 3-4) or 8 days in the same conditions (lanes 5-6 and 7-8, respectively), and from C2C12 myotubes cultured in 5 mM (lanes 9-10) or 25 mM glucose (lanes 11-12) were separated by SDS/PAGE, and succinated proteins were detected using a polyclonal anti-2SC antibody, as described in Experimental, (B) reprobed with anti-actin, (C) reprobed with anti-β-tubulin. (D) Coomassie blue staining of the blot shown in (A), (B) and (C), indicating the region where actin (black arrow), β-tubulin (empty arrow) and the 2SC labeled protein of interest were located. The actin content (~42 kDa) is significantly higher in C2C12 myotubes compared to 3T3 adipocytes (B, D), whereas tubulin levels were similar in both cell types (C, D). Molecular masses of marker proteins are indicated on the left-hand side.

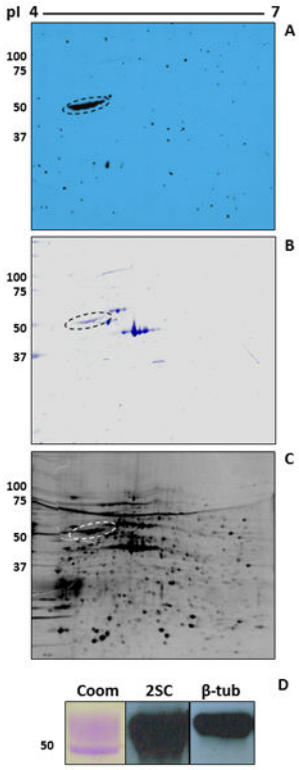

Figure 2.

Tubulin is the primary succinated protein in C2C12 myotubes. (A) Protein (400 μg) from C2C12 myotubes cultured in 25 mM glucose was analyzed by 2D gel electrophoresis across a 4-7 pH range as described in Experimental. Blots were probed with an anti-2SC antibody to detect succinated proteins. (B) Coomassie blue staining of the blot shown in (A). (C) Duplicate gel stained with Sypro Ruby. The 2SC blot (A) was used as a reference to excise the corresponding gel spot and the protein was identified by MALDI-TOF MS (Table 1). Note that the prominent succinated protein (dashed oval) in (A) corresponds to a mid-intensity protein spot both in the Coomassie (B) and the Sypro gel (C). Other prominent proteins in the Coomassie (B) and Sypro Ruby gel (C), including actin (~42 kDa), were not detected in the 2SC blot (A). (D) Protein (500 μg) from C2C12 myotubes cultured in 25 mM glucose was immunoprecipitated with an anti β-tubulin antibody. After treatment of the agarose beads with Laemmli buffer, half of the sample was electrophoresed and stained with Coomassie blue (Coom) to detect immunoprecipitated tubulin. The remainder was electrophoresed and transferred prior to probing with an anti-2SC antibody (2SC), followed by stripping and confirmation of the identity of the protein with an anti β-tubulin antibody (β-tub). Molecular masses of marker proteins are indicated on the left-hand side.

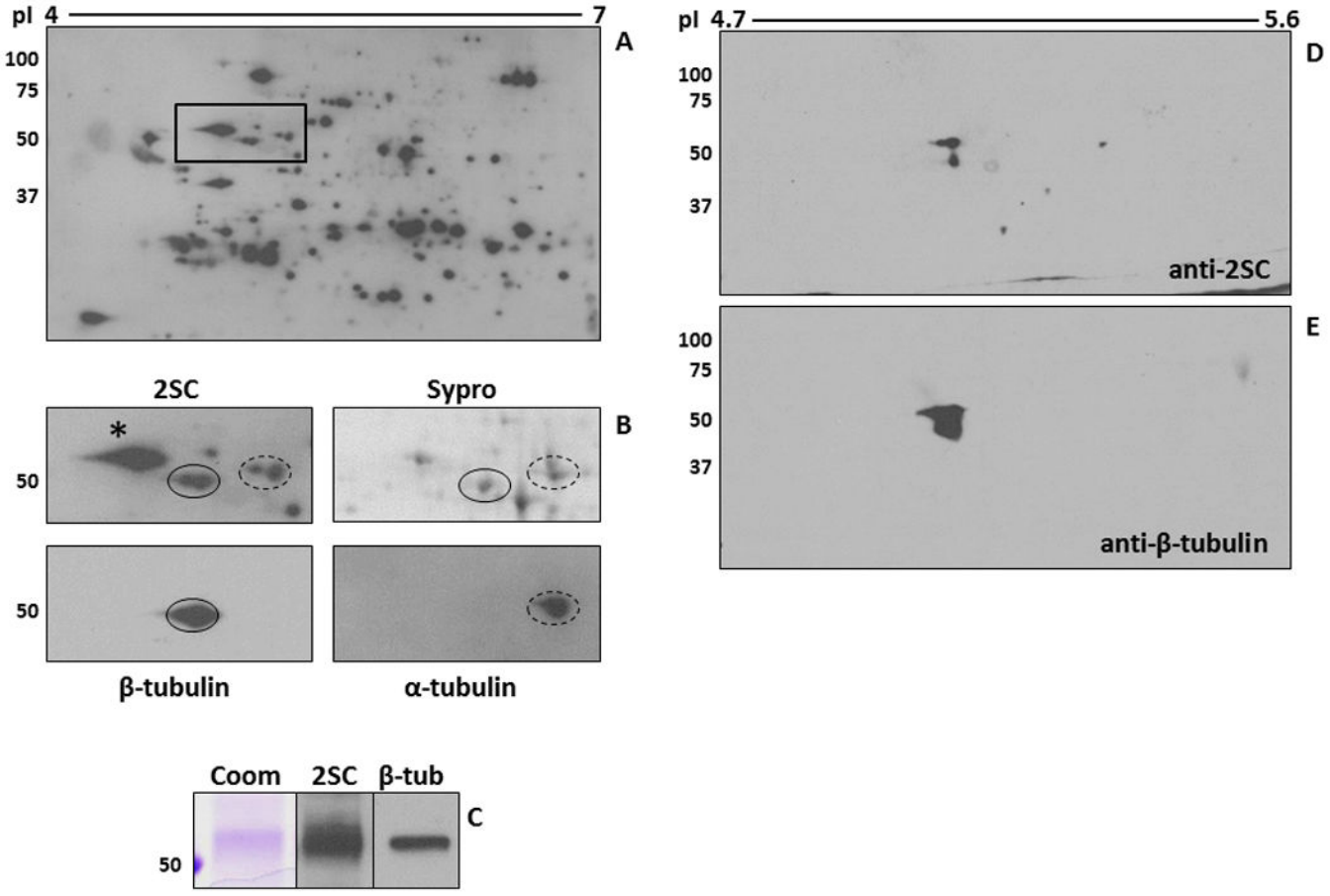

Figure 3.

Tubulin succination in 3T3 adipocytes cultured in high glucose medium. (A-B) Protein (500 μg) from 3T3 adipocytes grown in 30 mM glucose was analyzed by 2D gel electrophoresis across a 4-7 pH range. Duplicate gels were either transferred and immunoblotted with an anti-2SC antibody to detect succinated proteins (A, B-2SC), or stained with Sypro Ruby to observe total protein (B-Sypro). After detection of 2SC-modified proteins, the blot was stripped and probed sequentially with antibodies to α-tubulin (B-α-tubulin, dashed line) and β-tubulin (B-β-tubulin, solid line) in order to locate and excise the corresponding 2SC-modified spots in the Sypro Ruby-stained gel for identification (see Table 2). The images shown in panel B correspond to the rectangular area highlighted in panel A. * denotes another ∼50 kDa succinated protein which was identified as Protein Disulfide Isomerase. (C) Protein (500 μg) from 3T3 adipocytes grown in 30 mM glucose was immunoprecipitated with an anti β-tubulin antibody. After treatment of the agarose beads with Laemmli buffer, half of the sample was electrophoresed and stained with Coomassie blue (Coom) to detect immunoprecipitated tubulin. The remainder was electrophoresed and transferred prior to probing with an anti-2SC antibody (2SC), followed by stripping and confirmation of the identity of the protein with an anti β-tubulin antibody (β-tub). (D-E) An adipose tissue extract (200 μg of protein) from *db/db* mice was immunoprecipitated with an anti β-tubulin antibody and analyzed by 2D gel electrophoresis across a 4.7-5.9 pH range (4.7-5.6 range is shown). The gel was transferred and probed with an anti-2SC antibody (D), followed by

stripping and confirmation of protein identity with an anti β-tubulin antibody (E). Molecular masses of marker proteins are indicated on the left-hand side.

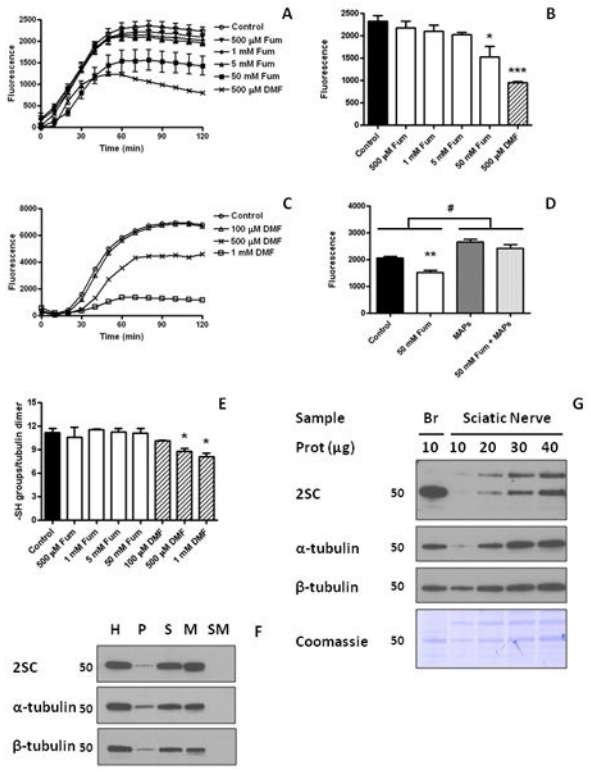

Figure 4.

Tubulin polymerization is inhibited by dimethyl fumarate. (A) Purified porcine brain tubulin was incubated for 24 h with increasing concentrations of fumarate (Fum, 500 μM to 50 mM) or with 500 μM dimethyl fumarate (DMF) and subjected to polymerization as described in Experimental, n=3 for each treatment. (B) Quantification of the tubulin polymerization assay shown in (A) at time = 90 min. Both 50 mM Fum and 500 μM DMF significantly decreased tubulin polymerization. (C) Purified porcine brain tubulin was incubated for 6 h with increasing concentrations of DMF (100 μM to 1 mM) and subjected to polymerization as described in Experimental, n=2 for each treatment. (D) Quantification at time = 90 min of purified porcine brain tubulin polymerization in the absence (No MAPs) or presence (MAPs) of microtubule associated proteins (tubulin to MAPs ratio 97:3), after a 24 h preincubation without (Cont) or with 50 mM fumarate (Fum). (E) The number of sulfhydryl (-SH) groups in pure porcine brain tubulin after *in vitro* polymerization was determined by the DTNB method as described in Experimental. n=3-5. Fum, from 500 μM to 50 mM did not change –SH group content of tubulin, whereas DMF decreased the number of –SH groups in tubulin at 500 μM and 1 mM concentrations. (F) Succinated mouse brain tubulin is incorporated into microtubule polymers. Brain extracts from control mice were subjected to tubulin polymerization as described in Experimental. Fractions of the initial homogenate (H), the first pellet (P), the first supernatant (S), the microtubular pellet obtained after polymerization (M), and the supernatant of the microtubular pellet (SM) were loaded based on volume (equivalent to 3 μg of the initial H fraction), resolved by SDS/PAGE, and transferred to a PVDF membrane. A 2SC-modified band of ∼50 kDa was detected in H, and after the initial centrifugation was concentrated in S (upper panel). After polymerization, the reactivity was present in the pellet (M) but not in the supernatant (SM). The distribution of

2SC modified proteins in the different fractions correlates with both α-tubulin (middle panel) and β-tubulin (lower panel). (G) Succination of tubulin is increased in brain compared to sciatic nerve. Brain (10 μg prot) and sciatic nerve (10-40 μg prot) extracts from control mice were resolved by SDS/PAGE and immunoblotted with anti-2SC antibody, prior to stripping and reprobing with α-tubulin and β-tubulin antibodies. Coomassie staining is also shown. Molecular masses of marker proteins are indicated on the left-hand side. In (A), (B), (D) and (E), results are expressed as mean ± SE; in (C) results are shown as the average. *: $p<0.05$; **: $p<0.01$; and ***: $p<0.001$ vs. Control; $^{\#}$: $p<0.001$ vs. No MAPs.

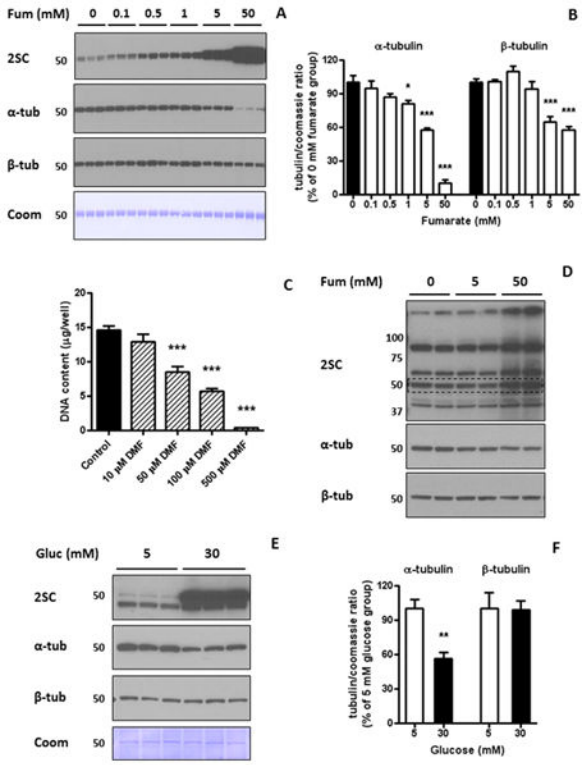

Figure 5.

Tubulin succination alters antibody binding capacity. (A) Samples of purified porcine brain tubulin subjected to *in vitro* polymerization (1 μg in triplicates) were resolved by SDS/PAGE and immunoblotted with anti-2SC antibody (2SC panel), and after stripping with α-tubulin (α-tub panel) and β-tubulin (β-tub panel). Tubulin succination increased with fumarate (Fum) concentration, while Coomassie staining (Coom panel) showed even loading of the lanes. (B) Quantification of the optical density of α-tubulin and β-tubulin bands relative to the Coomassie staining in (A), showing that α-tubulin and β-tubulin immunoreactivity decreased with Fum concentration (* $p<0.05$; *** $p<0.001$ vs. Control). (C) The DNA content of 3T3 fibroblasts in culture in the absence or presence of different concentrations of dimethylfumarate (DMF, 10-500 μM) was assessed by a cell proliferation assay, as described in Experimental. 50 μM, 100 μM and 500 μM DMF significantly decreased DNA content (*** $p<0.001$ vs. Control). (D) 3T3 fibroblasts in culture were treated with 5 mM or 50 mM Fum for 24 h. Cell extracts (30 μg of protein) were resolved by SDS/PAGE, and immunoblotted with an anti-2SC antibody (upper panel), showing that 50 mM Fum increased the intensity of several bands, including a ∼50 kDa protein (dashed line). After stripping, the same membrane was probed with antibodies against α-tubulin (middle panel) and β-tubulin (lower panel), showing a decrease in α-tubulin immunoreactivity. (E) Total cell lysates (20 μg protein) from 3T3 adipocytes matured in 30 mM vs. 5 mM glucose (Gluc) for 8 days were separated by SDS/PAGE. Tubulin succination (2SC panel) was increased on the ∼50 kDa band, while Coomassie staining (Coom panel) showed equal loading of the lanes. (F) Quantification of the optical density of α-tubulin and β-tubulin bands relative to the Coomassie staining in (E), showing that α-tubulin immunoreactivity was decreased in cells grown in 30 mM vs. 5 mM glucose (α-tub panel;

** $p<0.01$ vs. Control). In (A), (D) and (E), molecular masses of marker proteins are indicated on the left-hand side. In (B), (C) and (F) results are expressed as mean ± SE, with n=4 (B) or n=3 (C, F).

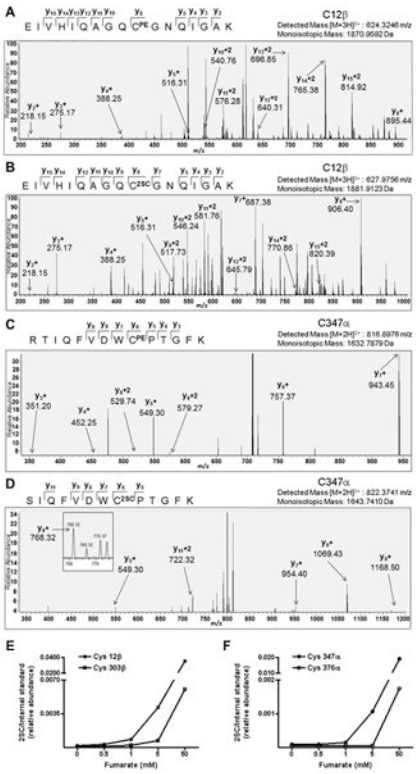

Figure 6.

Cys347 and 376 on α-tubulin and Cys12 and 303 on β-tubulin are prominent sites of succination. Purified porcine brain tubulin samples incubated in 0, 0.5, 1, 5 or 50 mM fumarate for 24 h were resolved by SDS/PAGE and the tubulin bands at ∼50 kDa were excised and digested with trypsin prior to LC-MS/MS analysis as detailed in Experimental. (A) MS/MS sequencing showing pyridylethylation of Cys12β (C^{PE}) in the peptide EIVHIQAGQCGNQIGAK in control unmodified tubulin. (B) MS/MS sequencing showing succination of Cys12β (C^{2SC}) in the peptide EIVHIQAGQCGNQIGAK in tubulin treated with 5 mM fumarate. (C) MS/MS sequencing showing pyridylethylation of Cys347α (C^{PE}) in the peptide RTIQFVDWCPTGFK in control unmodified tubulin. (D) MS/MS sequencing showing succination of Cys347α (C^{2SC}) in the peptide SIQFVDWCPTGFK in tubulin treated with 5 mM fumarate. In all cases only the y ions have been labeled for visual clarity. Both the detected mass and the theoretical mass are listed for each peptide. (E) Relative quantification of the extent of succination in the peptides containing Cys12 and Cys303 in β-tubulin and (F) Cys347 and Cys376 in α-tubulin were performed after normalization to the robust internal standard peptide YLTVAAVFR, ($[M+2H]^{2+}$, 520.2993).

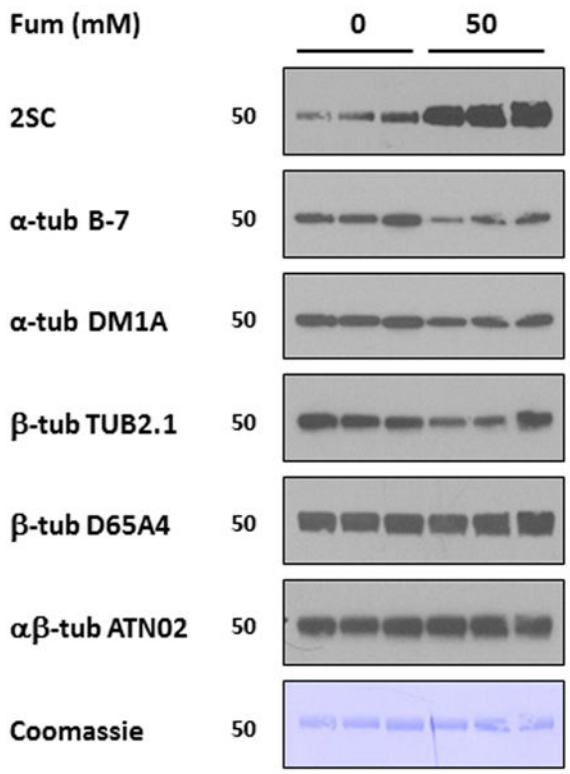

Figure 7.

Tubulin succination of specific residues decreases its immunoreactivity with tubulin antibodies. Samples of purified porcine brain tubulin (1μg in triplicates) incubated without (0) or with 50 mM fumarate (50) were resolved by SDS/PAGE and immunoblotted with anti-2SC antibody, stripped and subsequently probed with antibodies to (i) α-tubulin B-7; (ii) α-tubulin DM1A; (iii) β-tubulin TUB2.1; (iv) β-tubulin D65A4; and (v) αβ-tubulin ATN02; and finally stained with Coomassie blue. Note that the increase in succination in 50 mM fumarate corresponds with a decrease in tubulin immunoreactivity for some antibodies (B-7 and TUB2.1), but not for others (DM1A, D65A4 and ATN02), while Coomassie staining showed equal loading of the lanes. Molecular masses of marker proteins are indicated on the left-hand side.

Table 1

Summary of peptide mass fingerprinting data for all β-tubulin peptides identified, based on Mascot search results. M^{ox} = oxidized methionines, Mr = average mass

Peptide	Observed Mass	Mr (expt)	Mr (calc)	Sequence
47-58	1301.94	1300.94	1300.63	R.ISVYYNEATGGK.Y
104-121	1959.24	1958.24	1957.97	K.GHYTEGAELVDSVLDVVR.K
242-251	1130.77	1129.76	1129.59	R.FPGQLNADLR.K
242-252	1258.89	1257.88	1257.68	R.FPGQLNADLRK.L
252-262	1287.92	1286.92	1286.72	R.KLAVNM^{ox}VPFPR.L
253-262	1159.81	1158.8	1158.62	K.LAVNM^{ox}VPFPR.L
263-276	1621.06	1620.05	1619.83	R.LHFFMPGFAPLTSR.G
263-276	1637.06	1636.05	1635.82	R.LHFFM^{ox}PGFAPLTSR.G
310-318	1039.75	1038.75	1038.59	R.YLTVAAVFR.G
337-350	1697.07	1696.06	1695.83	K.NSSYFVEWIPNNVK.T
381-390	1245.79	1244.78	1244.59	R.ISEQFTAM^{ox}FR.R

Table 2

MS/MS peptide identification for tubulin spots. Data were processed using the MassLynx software package to generate peak list files (pkl) which were searched using Mascot. Mascot scores greater than 67 were considered significant ($p<0.05$).

Sample	Protein ID	Species	Swiss Prot #	Mass	Mascot Score	# Peptides Identified
5 mM glucose alpha tubulin spots	Tubulin alpha-2 chain	mouse	P05213	50152	208	8 (26%)
30 mM glucose alpha tubulin spots	Tubulin alpha-2 chain	mouse	P05213	50152	250	7 (25%)
	Tubulin alpha-1 chain	mouse	P68369	50136	110	7 (25%)
5 mM glucose beta tubulin spots	Tubulin beta-5 chain	mouse	P99024	49671	870	14 (37%)
	Tubulin beta-2C chain	mouse	P68372	49831	753	14 (37%)
	Tubulin beta-2A chain	mouse	Q7TMM9	49907	632	12 (32%)
	Tubulin beta-3 chain	mouse	Q9ERD7	50419	512	10 (27%)
	Tubulin beta-6 chain	mouse	Q922F4	50090	345	8 (20%)
30 mM glucose beta tubulin spots	Tubulin beta-5 chain	mouse	P99024	49671	809	13 (33%)
	Tubulin beta-2C chain	mouse	P68372	49831	739	13 (33%)
	Tubulin beta-3 chain	mouse	Q9ERD7	50419	575	9 (24%)
	Tubulin beta-2A chain	mouse	Q7TMM9	49907	573	10 (26%)
	Tubulin beta-6 chain	mouse	Q922F4	50090	416	7 (17%)

Table 3
Levels of 2SC in purified porcine brain tubulin

Group	2SC (mmol/mol Lys)
Control	0.227
50 mM Fum	10.814
500 μM DMF	495.255

Porcine brain tubulin (500 μg in duplicates) were incubated at 37°C for 24 h in phosphate buffer (pH 7.4) without any addition (Control) or with 50 mM fumarate (Fum) or 500 μM dimethyl fumarate (DMF). Samples were then analyzed by GC-MS/MS as described in Experimental and 2SC levels were expressed as mmoles 2SC/mole lysine. Mean values are shown.

Table 4

Succination sites (C^{2SC}) of purified porcine brain tubulin after treatment with 500 μM dimethyl fumarate (DMF). M^{ox} = oxidized methionine, PSMs = Peptide spectral matches.

Peptide Sequence	Swiss Prot #	Observed Mass	Succination Site(s)	PSMs
Tubulin alpha-1B peptides(Sus scrofa)	F2Z5T5			
$YM^{ox}AC^{2SC}CLLYR$		1400.6012	C315	16
$YMAC^{2SC}C^{2SC}LLYR$		1423.5927	C315, C316	1
$AYHEQLSVAEITNAC^{2SC}FEPANQM^{ox}VK$		2853.3174	C295	8
$TIQFVDWC^{2SC}PTGFK$		1685.7911	C347	5
$AVC^{2SC}M^{ox}LSNTTAIAEAWAR$		1967.9232	C376	16
Tubulin beta peptides (Sus scrofa)	P02554			
$EIVHIQAGQC^{2SC}GNQIGAK$		1909.9379	C12	5
$KEAESC^{2SC}DC^{2SC}LQGFQLTHSLGGGTGSGM^{ox}GTLLISK$		3629.6583	C127, C129	1
$LTTPTYGDLNHLVSATM^{ox}SGVTTC^{2SC}LR$		2811.3481	C239	5
$NMM^{ox}AAC^{2SC}DPR$		1168.4404	C303	15
$TAVC^{2SC}DIPPR$		1115.5402	C354	17